JOURNAL OF MATERIALS SCIENCE **36** (2001) 2865–2874

Morphology development of isotactic poly(4-methylpentene-1) during melt crystallization

C. SILVESTRE*, S. CIMMINO, E. DI PACE, M. L. DI LORENZO, G. ORSELLO
Istituto di Ricerca e Tecnologia delle Materie Plastiche. CNR. Via Toiano 6, 80072 Arco Felice (NA), Italy
E-mail: silv@irtemp.na.cnr.it

F. E. KARASZ
Department of Polymer Science and Engineering, University of Massachusetts, Amherst, MA, 01003, USA

J. S. LIN
Solid State Division, Oak Ridge National Laboratory, Oak Ridge, TN 37831, USA

The morphology of melt-crystallized isotactic poly(4-methylpentene-1) samples, prepared by varying crystallization temperature and time, as well as annealing temperature, has been probed by small and wide angle x-ray scattering, and electron microscopy. This was then correlated with the thermal properties investigated by differential scanning calorimetry. Relationships among melting behavior, morphological evidences and X-ray results have been found. Different populations of lamellae, grown with a time-dependent sequence, can be obtained: their relative amount and thermal stability is determined by crystallization and annealing conditions.

1. Introduction

Isotactic poly(4-methylpentene-1) (P4MP1) is a semicrystalline polyolefin with a bulky side group (CH_2-$CH(CH_3)_2$). P4MP1 presents several interesting properties [1–3], such as high chemical stability and low dielectric constant. Moreover P4MP1 is the only semicrystalline polymer in which the density of the amorphous fraction is lightly higher than the density of the crystalline fraction at room temperature. Several authors invoked the low packing density of the crystalline molecules to explain this unusual behavior [3]. Although semicrystalline, P4MP1 is transparent at room temperature as the crystal and amorphous densities are nearly equal [4]. P4MP1 is extensively employed for a number of applications, such as medical and chemical equipment, microwave oven cookware and food packaging [3].

Several authors have investigated the morphology of P4MP1 in order to interpret the interesting properties of this complex material [5–8]. Most of these studies have been described in comprehensive reviews by Lopez *et al.* [9] and by Silvestre *et al.* [10, 11]. It was underlined that the physical texture and the molecular arrangement within the material depend on crystallization conditions. Of particular inherent interest are the papers by Bassett and Patel [5, 6], who studied the melting behavior, morphology and isothermal lamellar thickening of P4MP1. They found that spherulites of P4MP1 crystallized from the melt developed from initial square lamellae by iteration of branching and divergence. This produced a framework of individual dominant lamellae, within which subsidiary lamellae developed. The melting point of the dominant lamellae was higher than that of the subsidiary lamellae. By annealing the crystallized sample at temperatures close to the melting point, the lamellae thickened isothermally, achieving higher stability and melting point.

The results of previous studies by some of us [12, 13] indicate the formation of one or two populations of lamellae, differing in thickness, depending on crystallization conditions. In particular, for non-isothermally crystallized samples, a single broad melting peak on DSC curves was present. For the isothermally crystallized samples two melting peaks were detected. They were attributed to two populations of lamellae with different thicknesses, formed in two stages of crystallization. The hypothesis that, depending on crystallization conditions, one or two populations of lamellae formed was also in agreement with some preliminary morphological and X-ray results [12].

Similar studies dealing the influence of crystallization condition on the morphology of several polymers were reported in the literature [14–18]. These studies constituted the basis for the interpretation of the results reported in the present paper.

* Author to whom all correspondence should be addressed.

This paper reports a complete study on morphology, superstructure and thermal behavior of P4MP1 samples crystallized over a wide range of preparation conditions.

2. Experimental part

2.1. Materials and preparation of the samples

The P4MP1 used in this study was obtained by Scientific Polymer Products Inc. with: $M_w = 6.0 \times 10^5$, $M_n = 6.5 \times 10^4$, density = 835 kg/m^3 and $T_g = 35 \pm 2$°C (measured by DSC).

P4MP1, as received, was compression-molded in a heated press at a temperature of 255°C for 5 minutes, without any applied pressure to allow complete melting. After this period, a pressure of 90 bar was applied for 6 min. Then the pressure was released and the mold was quenched in water at room temperature. The mold produced samples of 65 × 100 × 0.50 mm.

It is well known that P4MP1 degrades in presence of oxygen [3]. In this process of thermooxidative degradation, molecular mass is reduced with the formation of low molecular mass species. In order to exclude oxidation phenomena as a source of changes occurring during the molding procedure, TGA and FTIR experiments before and after the molding procedure were performed. The results indicated that the experimental conditions used during the compression molding do not produce detectable oxidation of the polymer.

P4MP1 samples were subjected to different thermal treatments conducted in a Mettler hot stage, under a dry nitrogen atmosphere. Each sample was heated from 30 to 290°C at 50°C/min, held at 290°C for 10 min, then rapidly cooled to the crystallization temperature, T_c, and kept at T_c for a time sufficient for crystallization. After crystallization, certain samples were subsequently annealed at the temperature T_a for different times, t_a. Temperatures and times of crystallization and annealing for all the samples are reported in Table I. After the thermal treatments, the samples were investigated by small angle X-ray scattering (SAXS), wide angle X-ray scattering (WAXS), scanning electron microscopy (SEM), and differential scanning calorimetry (DSC).

TABLE I Structural parameters of P4MP1 samples in dependence of crystallization and annealing conditions

Code	T_c (°C)	t_c (min)	T_a (°C)	t_a (min)	Δw (nm^{-1})	L(I) (nm)	L(II) (nm)	X_c (%)
1	180	15			0.132	70	27	60
2	220	40			0.74	70	38	64
3	180	15	220	20	0.94	70	33	57
4	180	15	220	40	0.94	70	33	57
5	180	15	220	120	0.94	70	32.5	59
6	180	15	220	180	0.94	70	33	60
7	180	15	222	120	0.85	70	34	58
8	180	15	225	120	0.84	70	35	59
9	180	15	227	40	0.82	70	45	56
10	180	15	227	120	0.80	70	45	59

Crystallization temperature (T_c), crystallization time (t_c), annealing temperature (T_a), annealing time (t_a), peak width of Lorentz-corrected SAXS profile (Δw), long period of type I lamellae (L(I)), long period of type II lamellae (L(II)), crystallinity fraction (X_c).

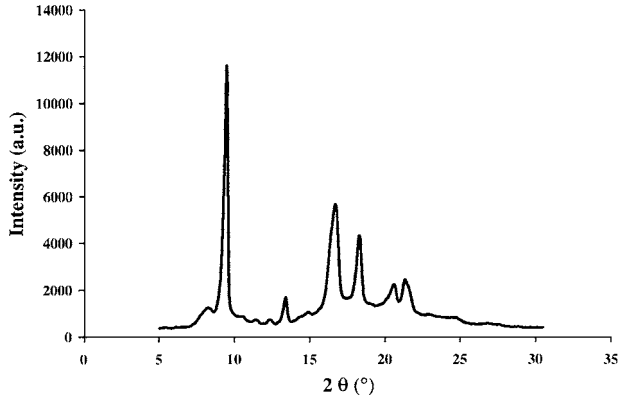

Figure 1 One-dimensional WAXS pattern for P4MP1 isothermally crystallized at 220°C for 40 minutes (sample 2).

2.2. Techniques

2.2.1. Wide angle X-ray scattering

Wide-angle X-ray scattering (WAXS) measurements were carried out on a Philips (PW 1050 model) powder diffractometer (CuNi-filtered radiation) equipped with a rotating sample holder device. The percentage crystallinity was computed by using the following procedure: On the WAXS diffractometer trace the background line was drawn between two points, which were chosen so that all diffraction patterns had minima at these points; the amorphous peak was sketched in somewhat arbitrarily, drawing a line connecting the two extreme minimum points of the baseline and the minima of the crystalline peaks; the ratio of the area under the crystalline peaks and above the amorphous peak to the total area above the background line, multiplied by 100, was taken as the P4MP1 percent crystallinity. A WAXS trace is shown for example in Fig. 1.

2.2.2. Small-angle X-ray scattering (SAXS)

The experiments were performed on the ORNL 10-m SAXS instrument with a sample-to-detector distance of 5.119 meters, using CuK_α radiation ($\lambda = 0.154$ nm) and a (200 × 200) mm^2 two-dimensional position-sensitive detector with each virtual cell element about 3 mm apart. The scattering intensity was stored in a 64 × 64 data array. Corrections were made for instrumental background, dark current due to cosmic radiation and electronic noise, and detector non- uniformity and efficiency (via a Fe^{55} radioactive standard, which emits γ-rays isotropically) on a cell-by-cell basis [19, 20]. The data were averaged in the q range $0.06 < q < 1.04$ nm^{-1}, [$q = (4\pi/\lambda)\sin(\theta/2)$, where λ is the X-ray wavelength and θ is the scattering angle], and converted to an absolute differential scattering cross section by means of pre-calibrated secondary standards.

The SAXS data were collected at $T = 100$°C as at room temperature the scattering is too low due to the similarity of the density between the amorphous and crystal phases.

The undetectable scattering at room temperature is a further, even if indirect, evidence that excludes oxidation of the sample during the molding. In fact the oxidation enhances greatly the low angle reflections of P4MP1 [21].

2.2.3. Scanning electron microscopy

The analyses of the surfaces were performed by using a SEM Philips XL 20 Series microscope on cryogenically fractured surfaces. Prior to the observation, the surfaces were etched by using the permanganate etching techniques, proposed by Olley and Bassett, to selectively remove the amorphous regions of the polyolefin [22]. Before the observation, the etched surfaces were coated with Au-Pd alloy with a SEM coating device (SEM BALTEC MED 020). The coating provides the entire sample surface with a homogeneous layer of metal of 18 nm $\pm$ 0.2 nm. The high uniformity of the thickness of the metal film excludes the possibility that the coating obliterated morphological details, like interfaces between lamellae.

In order to analyze the lamellar structure, micrographs at high magnification (30000×) were taken. As it was assumed that the lamellae were normal to the imaged plane, in order to obtain reliable values of the mean lamellar thickness, at least five samples crystallized at each given condition were scanned. Several micrographs were taken in different region of the sample. The mean values of the lamellar thickness are reported in the paper.

2.2.4. Thermal analysis

The calorimetric properties of the samples were investigated with a differential scanning calorimeter (Mettler DSC 30). The apparatus was calibrated with pure indium, lead and zinc at various scanning rates.

After the thermal treatment, each sample was heated from room temperature to 290°C at the rate of 10 °C/min. Some samples were also heated at 5°C/min. The heat evolved during the scanning process was recorded as a function of temperature.

During the heating dry nitrogen gas with a flow rate of 0.3 μm^3/sec was always purged through the cell.

3. Results

3.1. Structure

P4MP1 is a polymorph material with five crystalline modifications [23–25]. Crystallization from the melt generates the form known as modification I. This modification has a tetragonal cell with $a = b = 1.866$ nm and $c = 1.38$ nm. The WAXS pattern of P4MP1 did not change with the crystallization conditions used in this work, indicating that the polymer always crystallizes in modification I, (see Fig. 1).

The crystallinity content, X_c, obtained from WAXS patterns, is reported in Table I. For samples 1 and 2, crystallized at 180°C and 220°C respectively, without further annealing treatment, X_c are 60 and 64%, respectively. For the samples that undergo an annealing treatment after crystallization at 180°C, X_c slightly increases with time. It is interesting to note that X_c of the samples 1 and 2, is always higher than X_c of the sample annealed at 220°C after crystallization at 180°C, (samples 3 to 6), in agreement with the results reported in Ref. 12.

The Lorentz-corrected SAXS profiles for some representative samples are shown in Fig. 2. A hump at low angle and two peaks are present in all the samples, suggesting probably the presence of different types of lamella populations. The hump (that will be called first peak), whose position does not change with preparation condition, is centered at about $q = 0.09\ nm^{-1}$. The form and position of the other two peaks (called second and third peak) depend on thermal history. It is interesting to note that the ratio of the Lorentz-corrected scattering angle, for the third maximum to that of the second one, is close to 2, indicating that these two peaks are order maxima arising from the same structure.

The long periods relative to the first peak, L(I), and to the second peak, L(II), are calculated from the equation $L = 2\pi/q^*$, where q^* is the value of q at the peak in the Lorentz-corrected q^2 I(q) versus q plot. The values of L(I) and L(II) for all samples are reported in Table I.

The finding of two long periods could indicate the presence of two populations of lamellae. One population has a very high value of the long period, L(I) = 70 nm, that is independent of crystallization conditions used, as shown in Table I. The other one presents a lower long period, L(II), sensitive to the variation of crystallization temperature, T_c, annealing temperature, T_a, and annealing time, t_a.

Fig. 3 shows the dependence of L(II) on annealing temperature, for a given t_a. The samples (1, 5, 7, 8 and 10) were crystallized at 180°C for 15 minutes and annealed at the indicated temperature for 120 minutes. L(II) is markedly dependent on T_a especially at high T_a. In fact an increase of T_a of only 7 degrees, from 220 to 227°C, leads to an increase of L(II) of 12.5 nm.

The effect of annealing time on L(II) is reported in Fig. 4. The samples with the full circle symbols were crystallized at 180°C for 15 minutes, and then annealed at 220°C for the specified time (samples 1, 3, 4–6). On the same plot the value of L(II) for a sample crystallized at 220°C for 40 minutes is also reported, (full square symbol, sample 2). It is seen that twenty minutes of annealing at 220°C produce an increase of 6 nm in L(II). By holding the sample at 220°C for additional time, up to 3 hrs, no further thickening of the lamellae is detected, and the values of L(II) obtained for isothermally crystallization at 220°C is never reached (sample 2).

The heterogeneity of the lamellar distribution in the structure responsible of the second peak in the Lorentz plots can be determined by examining the peak width, Δw, measured at half height of the Lorentz-corrected SAXS profiles. The values of Δw for all samples are reported in Table I. Sample 1, crystallized at 180°C, yields the largest peak width, $\Delta w = 0.132\ nm^{-1}$, suggesting that a broad distribution of lamella thickness is present in this sample. This is due to the fact that at 180°C crystallization is not completely isothermal, as reported in Ref. 12. When the sample crystallized at

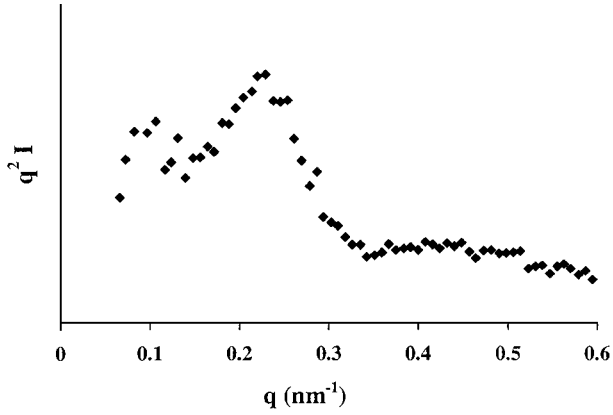

(a)

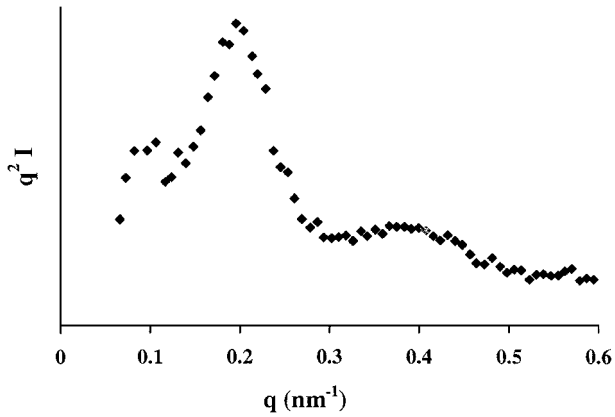

(b)

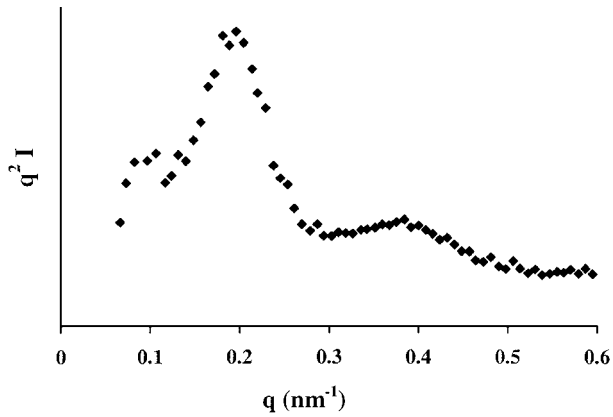

(c)

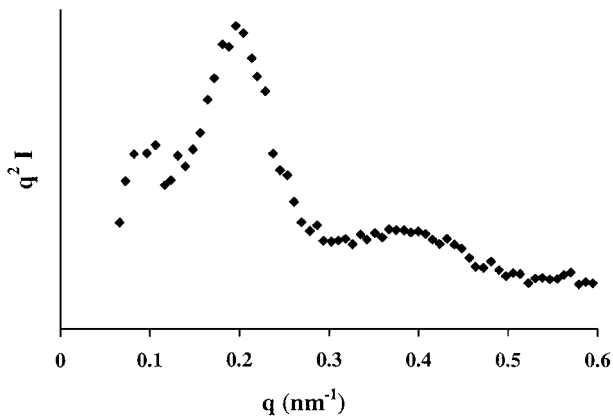

(d)

Figure 2 Lorentz-corrected SAXS profiles for samples of P4MP1 subjected to different thermal treatment: (a) sample 1, (b) sample 3, (c) sample 5, (d) sample 8.

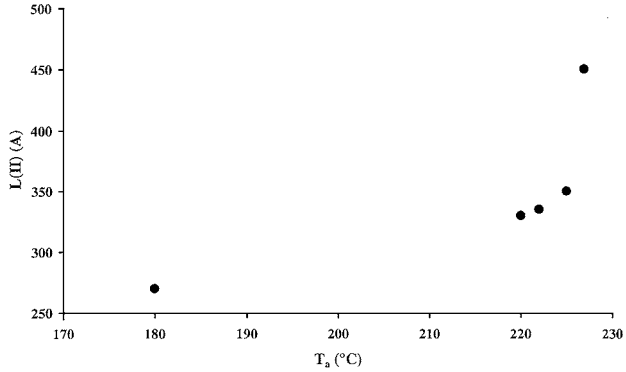

Figure 3 Long period, L(II), calculated from the second maximum in the Lorentz corrected plot as a function of annealing temperature. The samples before the annealing were crystallized at $T = 180°C$. The annealing time was of 120 minutes.

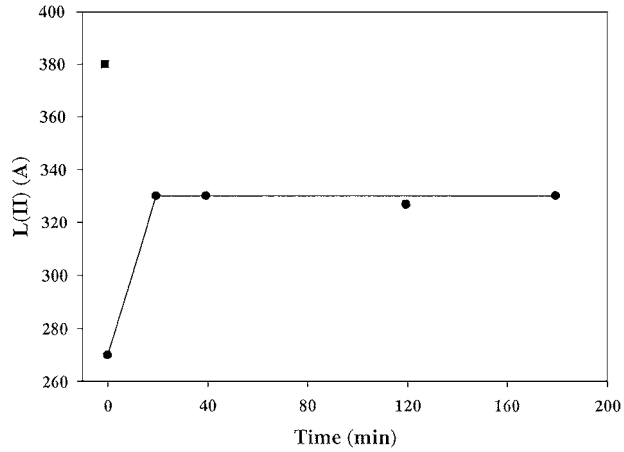

Figure 4 Long period, L(II), calculated from the second maximum in the Lorentz corrected plot as a function of annealing time, full circles. The sample were crystallized at $T = 180°C$ and annealed at 220°C. L(II) relative to the sample 2 crystallized at 220°C is also reported for comparison, square symbol.

180°C is annealed at 220°C for 20 min. (sample 3), Δw decreases to 0.93 nm^{-1}. For longer annealing times, Δw does not change any more (samples 4, 5 and 6). The results obtained indicate that the annealing at 220°C of the samples crystallized at $T = 180°C$ produces crystals with a narrower distribution of lamellae, and that the annealing process is completed in 20 minutes, in agreement with the results shown in Fig. 4. For the samples annealed at higher T_a (samples 7 to 10), the peak width is a function of annealing temperature and decreases with T_a.

3.2. Morphology

Independently of processing conditions, the crystallized samples are composed of spherulites with diameters of ca 30 μm, as illustrated in Fig. 5. Most of the spherulites are probably nucleated at the same time as inferred by the linear boundaries between them [26]. The leaf shape produced at an early stage is clearly revealed. Of particular note are the lamellar continuity along the radius (see Fig. 5b), the branching and divergence of lamellae and the square spirals revealed by the etching procedure (see Fig. 5c). Bassett and Patel

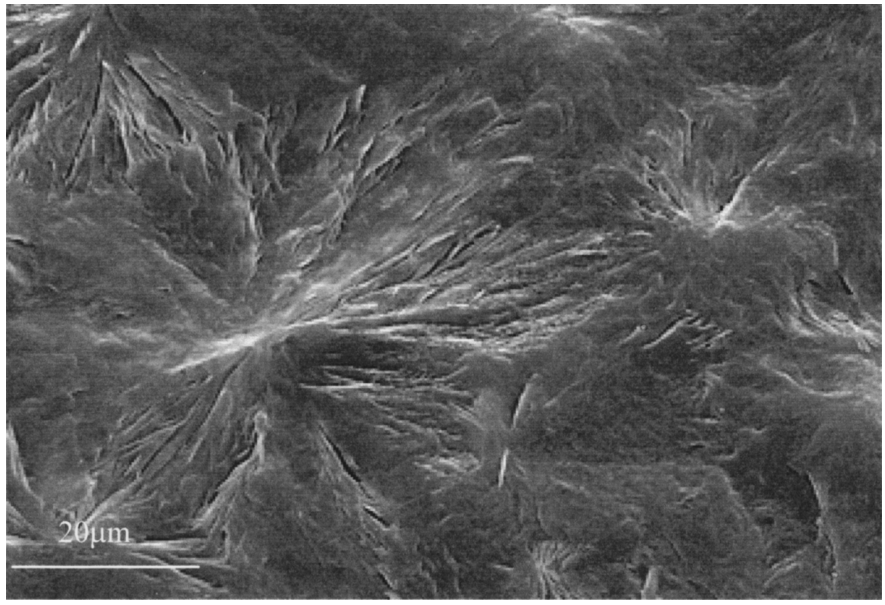

(a)

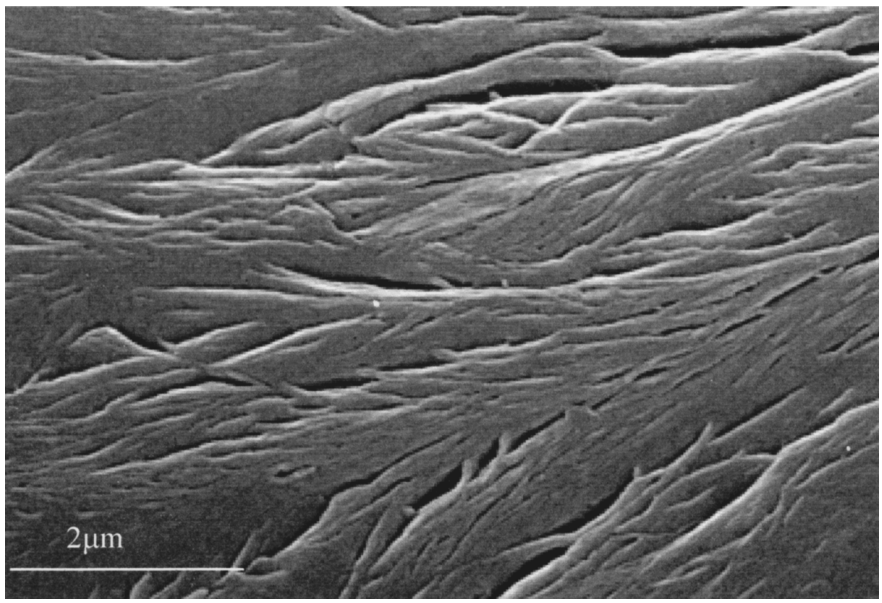

(b)

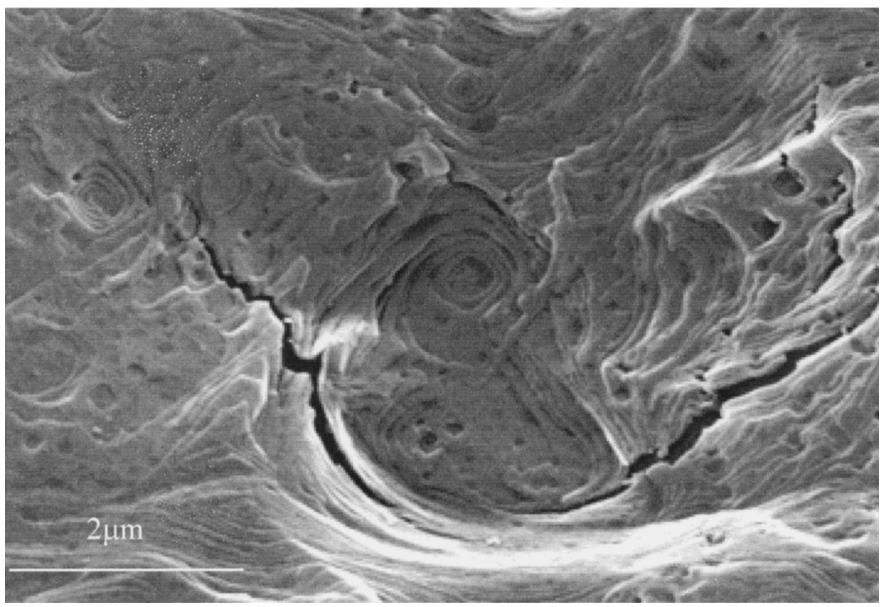

(c)

Figure 5 Scanning electron micrographs of surfaces of samples after etching: (a) and (b) sample 6; (c) sample 2. Different features can be noted: (a) P4MP1 crystallizes according to a spherulite morphology; the boundary between the spherulites is linear; (b) There is lamellae continuity along the radius; (c) Square spirals left by the etching are clearly visible.

reported similar morphological features in their study on morphology and crystallization of P4MP1 [5, 6].

A few thick lamellae are always present in all samples (type I lamellae), Fig. 6. Some of these lamellae grow forming a cross. Their thickness, measured on SEM micrographs, ranges between 50 and 60 nm, independently of crystallization and annealing conditions. Most of the sample surface is occupied by thinner lamellae (type II lamellae), Fig. 7. The width of type II lamellae ranges between 23 nm and 35 nm depending on crystallization conditions. In particular the thickness increases with crystallization and annealing temperatures.

For samples obtained by crystallization at 180°C and subsequent annealing, the thickness of type II lamellae increases with annealing temperature. For the samples crystallized at 180°C, (Fig. 7a) the type II lamellae have average thickness of 23 nm, whereas for the samples crystallized isothermally at 220°C (Fig. 7b) the lamellae are 35 nm thick. An increase of annealing time does not produce any further thickening. In no case did the lamellae annealed after solidification at 180°C reach the dimension of the lamellae obtained by isothermal crystallization at $T_c = T_a$, in agreement with the X-ray results, (compare Fig. 6 with Fig. 7b).

The presence of different populations of lamellae is also proved by preliminary results of an AFM study that we are carrying on. An AFM micrograph of a P4MP1 sample isothermally crystallized at 220°C is reported in Fig. 8. In the micrograph two populations of lamellae are clearly seen. The thickness of these lamellae is in good agreement with that measured on SEM micrographs. To note that all the micrographs report surface morphology and they might not be completely representative of the morphology of the material in the bulk.

3.3. Melting behavior

The melting behavior of polymer crystals depends on lamellar thickness, size of the crystals, perfection of molecular packing inside the lattice, and defect structure and distribution [27]. Moreover, since crystallization of a polymer is a kinetically controlled process, its melting depends upon crystallization rate and chain mobility. Hence the melting behavior, compared with the morphologies detected by electron microscopy and the structures obtained by small angle X-ray scattering, could provide additional global information on crystal populations.

Differential scanning calorimetry was used to study the melting behavior of the samples obtained in different conditions. After the thermal treatment reported in Table I, all the samples were heated from room temperature at 10°C/min to 290°C. Fig. 8 shows the DSC traces of representative samples relative to this melting scan. Fig. 9 shows the DSC traces of sample 4 heated at 5°C/min. In Fig. 8 one or two melting peaks and additional shoulders are detectable depending on crystallization conditions. The main peak is always centered at about $T = 241°C \pm 2$.

For the samples that do not undergo any annealing treatment, the results confirm the observations reported in our previous paper cited in the introduction [12]. For sample 1, for which crystallization is not isothermal, a single broad endotherm is observed. For sample 2, isothermally crystallized at 220°C, an additional melting peak at lower temperature is present. This peak starts at a temperature lower than T_c. For the annealed samples (3 to 10), the lower peak temperature disappears and shoulders are present, see Fig. 9. In Fig. 10 three melting peaks are present at about 225°, 232° and 240°C.

The correlation among morphological and X-ray results and the melting behavior is not immediately obvious, but carefully analyzing the data a complete and complex picture of the morphology of melt crystallized P4MP1 results. In fact as will be discussed in detail in the following sections, in the light of the results obtained, the melting behavior can be explained by hypothesizing that, together with lamellae type I and II, another population of lamellae (lamellae type III) could, in some cases, form non-isothermally during cooling from T_c to room temperature. Following this hypothesis the lower melting peak, present in sample 2, would be due to the melting of type III lamellae.

The melting peaks of these different lamellae populations are evident in Fig. 10 that reports the DSC trace of sample 4 heated at 5°C/min. Three peaks are present. The peak at low temperature could be due to the melting of lamellae type III. The peak at intermediate temperature probably is connected with the melting of lamellae type II and finally the peak at high temperature with lamellae type I.

For both heating rates some reorganization of the lamellae during the scanning could not be excluded, so the ratios of the peak area in the DSC traces are not indicative of the content of the different types of lamellae present at T_c.

We note that for linear and branched polyethylene quenched from the melt, Mandelkern and co-workers have reported a similar thermal behavior, that was attributed to the formation of random lamellae not organized into any well defined structure [28, 29].

4. Discussion

On the basis of the experimental results reported, the following hypothesis can be put forward. Few thick lamellae form under any crystallization conditions (type I lamellae). Probably these lamellae grow first. As their thickness and melting temperature is independent of crystallization conditions, they nucleate and grow at the same temperature (higher than T_c) during cooling from T_m to the established T_c. In order to verify this hypothesis, a study of the crystallization process of P4MP1 at temperature close to T_m is in progress, that together with a X-ray *in situ* crystallization are the subject of a forthcoming paper.

Once the sample has reached the established T_c, other lamellae (type II lamellae) grow isothermally. These lamellae are also visible on the micrographs of the etched samples and are responsible for the second and third maxima present on X-ray scattering patterns. Their melting occurs a few degrees below the main melting peak.

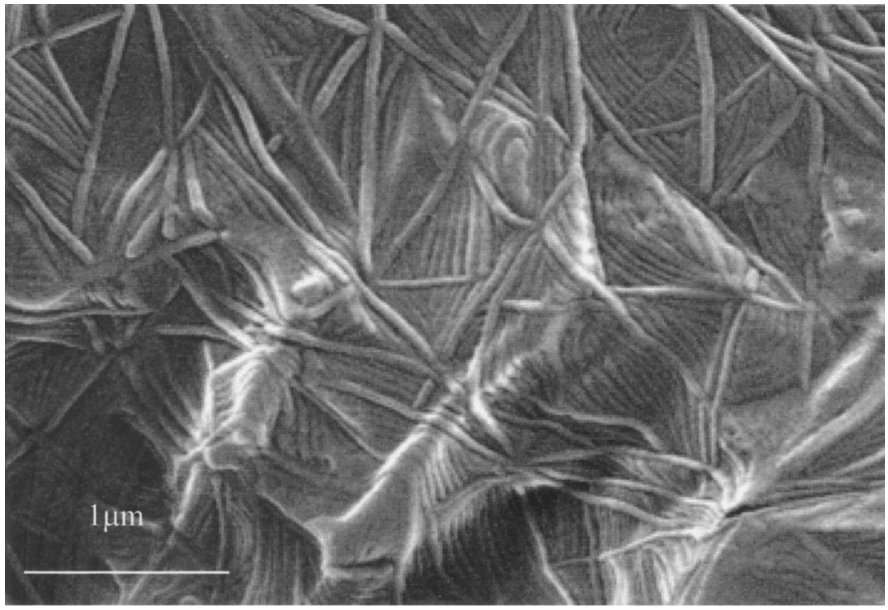

(a)

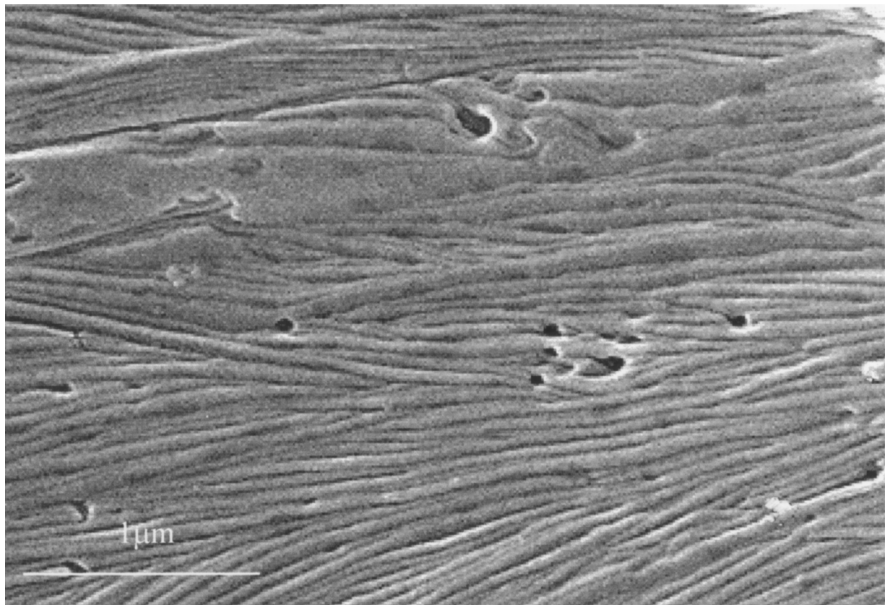

(b)

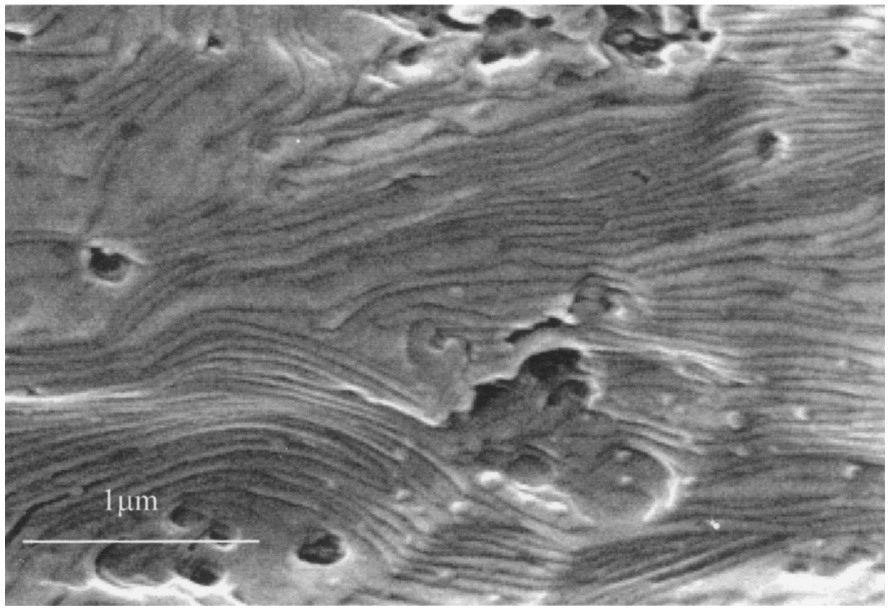

(c)

Figure 6 Scanning electron micrographs of surfaces of samples after etching: (a) sample 9, (b) and (c) sample 2. Very thick lamellae (type I lamellae) and thick lamellae (type II lamellae) are clearly seen.

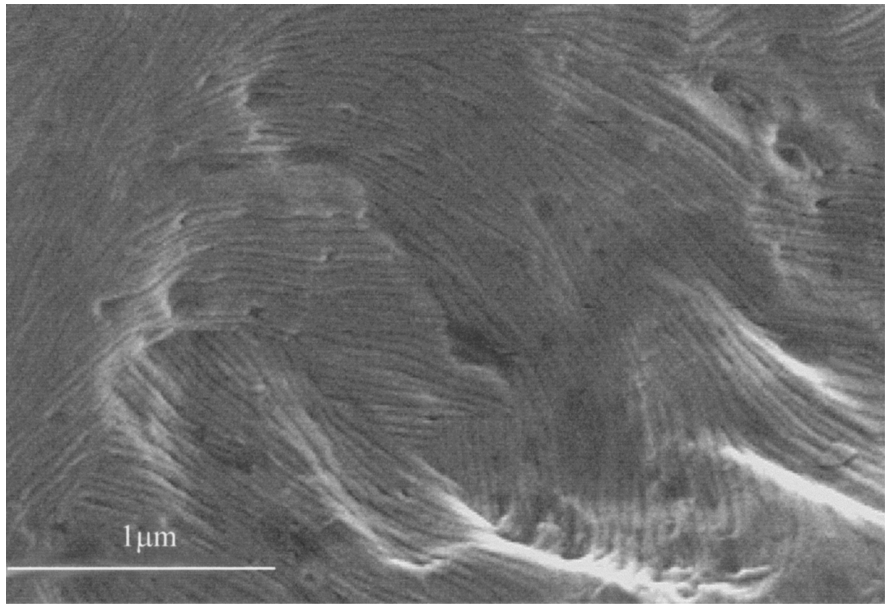

(a)

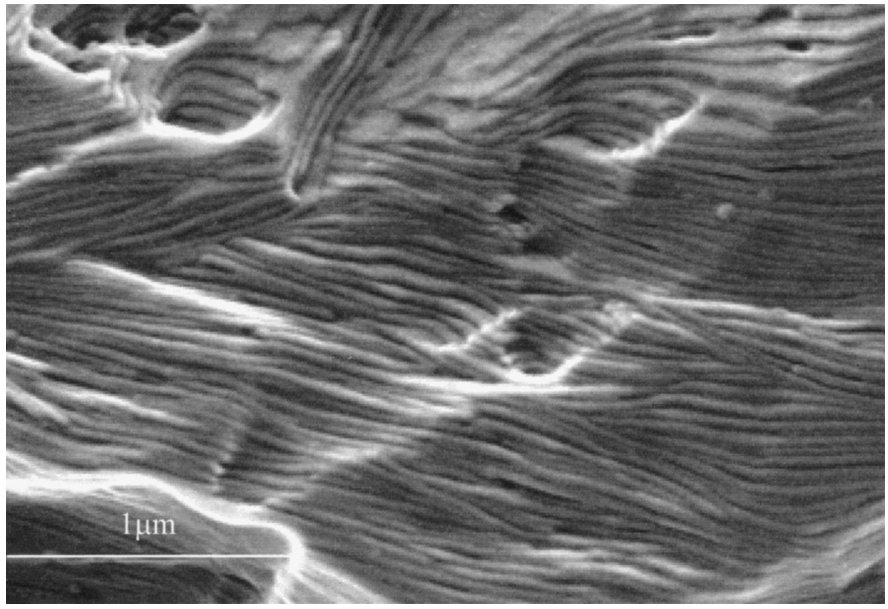

(b)

Figure 7 Scanning electron micrographs of surfaces of samples after etching. (a) sample 1; (b) sample 2. The increase of lamellar thickness with crystallization temperature is shown.

After cooling the isothermally crystallized samples to room temperature, a third type of lamellae, thinner than type I and II, probably form (type III lamellae). The presence of these lamellae can be hypothesized from the presence of a melting peak at lower temperature. To support this hypothesis we can consider that the scattering of these lamellae could be hidden under the second and third peak tail at higher q of the SAXS profiles (see Fig. 2). Type III lamellae were not observable on the micrographs of the etched samples, probably because, being defective and thinner, they were washed away by the etching, together with the amorphous material [5, 6]. In order to prove the existence of type III lamellae, an atomic force microscopy study of non-etched samples is in progress.

The formation of type III lamellae can be avoided by changing the crystallization conditions. In fact, the samples crystallized at $T_c = 180$ and annealed at 227°C do not yield, in the heating scan from room temperature, the melting peak at low temperature, indicating the absence of type III lamellae, as reported in Ref. 12.

The annealing at temperature higher than 220°C for different times of the samples crystallized at 180°C causes the melting of type III lamellae and the reorganization of type II lamellae, whereas the most stable type I lamellae remain unchanged. These effects account for the peaks, the shoulders and the constancy of the main melting peak observed in the DSC curves. In fact at 220°C type III lamellae melt; part of this melt material probably crystallizes again forming thicker lamellae, whereas type II lamellae do not melt, but undergo annealing phenomena, increasing their thickness at the expense of the surrounding melt material. In our samples this reorganization process is completed in twenty minutes. For longer t_a, in fact L(II) and the SAXS peak width, (Δw), are no longer functions of annealing time. This behavior could be attributed to the low packing density of crystalline P4MP1 molecules,

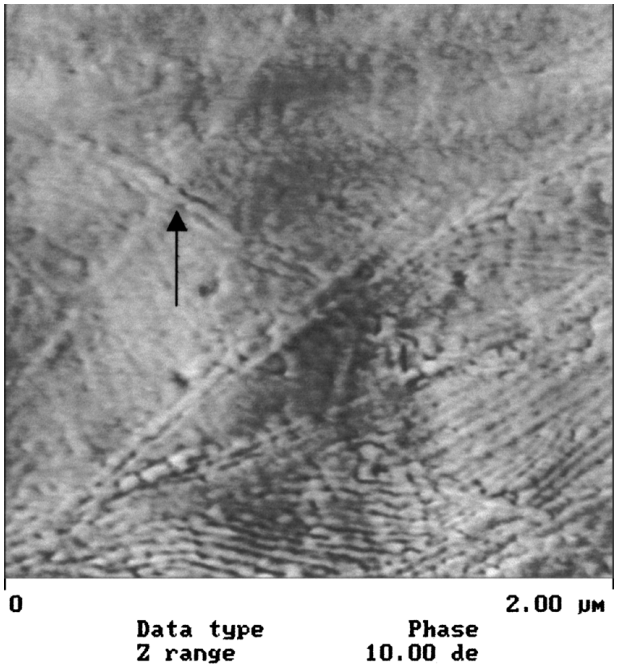

Figure 8 AFM micrograph of the surface of sample 2. Two populations of lamellae are clearly discernable: Few very thick lamellae, forming a cross (lamellae type I) are indicated with the arrow. Their thickness is about 50 nm; Several thinner lamellae with mean thickness of 25 nm (lamellae type II) are visible on the right bottom.

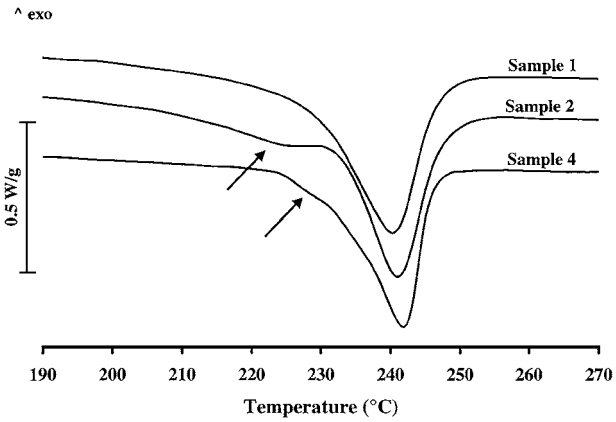

Figure 9 DSC traces of three representative samples. Heating rate 10°C/min.

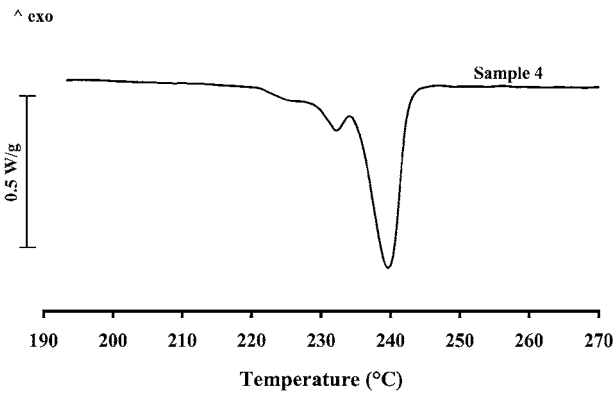

Figure 10 DSC trace of sample 4 heated at 5°C/min.

which produces high mobility at the annealing temperature. If we suppose that at T_a the annealing process of P4MP1 is controlled mainly by diffusion, the high chain mobility of the chains favors the reorganization, that is very rapid and complete in less than 20 minutes. Rybnikar and Geil obtained similar results studying the lamellar structure of P4MP1 crystallized from the melt in the 201–235 °C temperature range [7]. They found that the lamellar thickness was 35 nm independently of crystallization temperature and that the annealing did not change the mean lamellar thickness. Conversely, Bassett and Patel found that the lamellar thickness increased with the annealing time for samples crystallized at 231°C and kept at 241°C up to 1000 minutes [5]. The different behavior could be due to the different annealing temperature used.

It is important to note that the dimensions of the type II lamellae of the annealed samples never reach the value of L(II) of sample 2, that was isothermally crystallized at $T_c = T_a = 220$°C. Also the crystallinity of the annealed samples does not reach the values of the crystallinity of the sample isothermally crystallized at $T_c = 220$°C. This could indicate the importance of the environment in the annealing process of P4MP1. The type II lamellae of samples 3 to 10 are thinner than the same kind of lamellae of sample 2 as a consequence of the difficulties of forming lamellae in the environment of previously formed lamellae. This difficulty produces also samples with lower crystallinity content.

5. Conclusions

The principal finding is that in melt crystallized P4MP1 various populations of lamellae with different thickness can be obtained depending on crystallization conditions.

In particular three types of lamellae can in some cases form: very thick lamellae (type I lamellae), whose thickness is independent of annealing and crystallization conditions used; thick lamellae formed at T_c (type II lamellae); irregular and thinner lamellae formed during cooling from T_c to room temperature, (type III lamellae).

We suppose that there is a time-dependent sequence of crystallization. As the material is cooled from the melt, few very thick lamellae (type I lamellae) start to grow. At T_c part of this melt material crystallizes forming thick lamellae (type II lamellae). Cooling the material to room temperature, additional material can crystallize, giving rise to very thin and defective lamellae. The type I lamellae are very stable and do not undergo any thickening at the used T_a. Their thickness is independent of crystallization and annealing conditions used. The thickness of type II and III lamellae is, conversely, strongly dependent on the preparation conditions.

This work, on one side, has substantiated the hypothesis already reported in reference 12, that for P4MP1 different populations of lamellae can be obtained changing the crystallization conditions.

On the other side the paper claims some novel effects:

1. identification of a lamellae population whose thickness is independent of crystallization and annealing conditions used;
2. identification of lamellae populations with different dependence of lamellar thickness on annealing time;
3. importance of the environment in the annealing process of P4MP1.

These effects, that seem in some contrast to long standing experience evidences, need in our opinion to be given attention with further studies. The authors, in order to have a complete pattern of the morphology of P4MP1, intend to study the crystallization process of P4MP1 at crystallization and annealing temperature close to T_m, following the structure development with X-ray *in situ* crystallization studies and analyzing the morphology also by using AFM techniques.

Acknowledgements

The research using SAXS analysis was supported in part by the Division of Materials Science, U.S. Department of Energy under Contract No. DE-AC05-96OR22464 with Lockheed Martin Energy Research Corp. One of the authors, C.S., likes to thanks the NATO-CNR Senior Fellowship Programme 1998 for financial support. The authors are indebted to Dr. Maria Errico and Mr. Emanuele Fiore for the FTIR and TGA analysis respectively.

References

1. K. J. KUMBHANI and E. G. KENT, in "Advances in Polymer Blends and Alloys Technology, Vol. II." edited by M. A. Kohudic, (Tecnomic Publishing Co. Inc., 1988).
2. A. C. PULEO, D. R. PAUL and P. K. WONG, *Polymer* **30** (1989) 1357.
3. Y. V. KISNIN, in "Encyclopedia of Polymer Science and Engineering," Vol. 9, edited by H. F. Mark and N. M. Bikales (J. Wiley and Sons: New York, 1987) p. 707.
4. F. L. SAUNDERS, *J. Polym. Sci., Polym. Lett. Ed.* **2** (1964) 755.
5. D. C. BASSETT and D. PATEL, *Polymer* **35** (1994) 1855.
6. D. PATEL and D. C. BASSETT, *Proc. R. Soc. Lond.* **A 445** (1994) 577.
7. F. RYBNIKAR and P. H. GEIL, *J. Macromol. Sci. Phys.* **B7** (1973) 1.
8. J. H. GRIFFITH and B. G. RANBY, *J. Polym. Sci. Polym. Phys. Ed.* **19** (1981) 1865.
9. L. C. LOPEZ, G. L. WILKES, P. M. STRICKLEN and S. A. WHITE, *J. Macr. Sci., Rev. Macromol. Chem. Phys.* **C32** (1992) 301.
10. C. SILVESTRE, M. L. DI LORENZO and E. DI PACE, Crystallization of Polyolefins in "Handbook of Polyolefins," 2nd ed., edited by C. Vasile (Marcell Dekker: New York, 2000) p. 223.
11. C. SILVESTRE, S. CIMMINO and E. DI PACE, Morphology of Polyolefins, in "Handbook of Polyolefins," 2nd ed., edited by, C. Vasile (Marcell Dekker: New York, 2000) p. 175.
12. C. SILVESTRE, S. CIMMINO, E. DI PACE and M. MONACO, *J.M.S.—Pure Appl. Chem.* **A35** (1998) 1507.
13. S. CIMMINO, M. MONACO and C. SILVESTRE, *J. Polym. Sci., Part B, Polym. Phys.* **35** (1997) 1269.
14. B. WUNDERLICH, "Macromolecular Physics," Vol. I (Academic Press, New York, 1976).
15. H. ZHOU and G. L. WILKES, *Polymer* **38** (1997) 5735.
16. I. G. VOIGT-MARTIN and L. MANDELKERN, *J. Polym. Sci., Part B, Polym. Phys* **22** (1984) 1901.
17. S. Z. D. CHENG, J. J. JANIMAK, A. ZHANG and E. T. HSIEH, *Polymer* **32** (1991) 648.
18. D. C. BASSETT, R. H. OLLEY and I. A. M. AL RAHEIL, *Polymer* **29** (1988) 1745.
19. G. D. WIGNALL, J. S. LIN and S. SPOONER, *J. Appl. Cryst.* **23** (1990) 241.
20. T. P. RUSSELL, J. S. LIN, S. SPOONER and G. D. WIGNALL, *J. Appl. Cryst.* **21** (1988) 629.
21. D. C. BASSETT, "Principles of Polymer Morphology" (Cambridge University Press: Cambridge, 1981).
22. R. H. OLLEY and D. C. BASSETT, *Polymer* **23** (1982) 1707.
23. H. KUSANAGI, M. TAKASE, Y. CHATANI and H. TADOKORO, *J. Polym. Sci.–Polym. Phys. Ed.* **16** (1978) 131.
24. F. C. FRANK, A. KELLER and A. O'CONNOR, *Philos. Mag.* **8** (1959) 200.
25. W. BASSI, O. BONSIGNORI, P. G. LORENZI, P. PINO, P. CORRADINI and P. A. TEMUSSI, *J. Polym. Sci.–Polym. Phys. Ed.* **9** (1971) 193.
26. A. E. WOODWARD, "Understanding Polymer Morphology" (Hanser Publishers, Munich, 1995).
27. B. WUNDERLICH, "Macromolecular Physics," Vol. 3, Crystal Melting (Academic Press, New York, 1980).
28. L. MANDELKERN, M. GLOTIN and R. A. BENSON, *Macromolecules* **14** (1981) 22.
29. F. SAKAGUCHI, J. MAXFIEL and L. MANDELKERN, *J. Polym. Sci., Polym. Phys. Ed.* **14** (1976) 2137.

Received 30 August
and accepted 28 November 2000